Homodimerization of presenilin N-terminal fragments is affected by mutations linked to Alzheimer's disease

Sara Cervantes, Roser Gonzàlez-Duarte, Gemma Marfany*

Departament de Genètica, Facultat de Biologia, Universitat de Barcelona, Avda. Diagonal 645, 08028 Barcelona, Spain

Received 14 May 2001; revised 24 July 2001; accepted 24 July 2001

First published online 14 August 2001

Edited by Gianni Cesareni

Abstract Mutations on human presenilins 1 and 2 cause dominant early-onset familial Alzheimer's disease (FAD). Presenilins are polytopic transmembrane proteins endoproteolytically processed in vivo to N- and C-terminal fragments (NTFs and CTFs). The functional presenilin unit consists of a high molecular weight complex that contains both fragments. Here we show NTF:NTF, CTF:CTF and NTF:CTF interactions by yeast two-hybrid and in vivo endoplasmic reticulum split-ubiquitin assays. Our results also highlight the involvement of HL1 – the hydrophilic loop between TMI and TMII – in the NTF:NTF binding site. Besides, nine FAD-linked presenilin mutations substantially affected HL1:HL1 binding. From the evidence of NTF and CTF homodimerization, we propose the contribution of two NTFs and two CTFs, instead of a single NTF:CTF heterodimer, to the functional presenilin–γ-secretase complex and that FAD mutations affect the assembly or stability of this complex.

Key words: Presenilin complex; Alzheimer's disease; Familial Alzheimer's disease mutation; γ-Secretase; Split-ubiquitin system; *Drosophila*

1. Introduction

Alzheimer's disease (AD) is the major neurodegenerative dementia syndrome in humans. Although it has a complex aetiology, a small proportion of AD cases show autosomal dominant inheritance. Mutations in three genes, the amyloid precursor protein (APP) and two members of the presenilin family, PS1 and PS2, cause early-onset AD (also called familial AD or FAD) [1,2]. Presenilins are polytopic transmembrane proteins, primarily located in the endoplasmic reticulum (ER) and early Golgi [3], which show a high degree of evolutionary conservation. Although the precise role of presenilins has not yet been established, biochemical and biological studies suggest their involvement in many crucial cellular processes such as calcium homeostasis, protein folding and trafficking, GSK-3β and tau metabolism, neuronal apoptosis and γ-secretase cleavage of APP and Notch ([4,5] and references therein).

PS1 and PS2 are predominantly found in vivo as ~27–28 kDa N-terminal (NTF) and ~16–17 kDa C-terminal (CTF) fragments. Full-length presenilin polypeptides are short-lived molecules, rapidly degraded via proteasomes, in contrast to NTFs and CTFs, which are much more stable [6]. The generation and accumulation of NTFs and CTFs are highly regulated. Both fragments build up to saturable levels at 1:1 stoichiometry, even when over-expressed [7,8]. In addition, full-length presenilins contribute to low molecular weight complexes (180 kDa), which develop into larger aggregates (250 kDa) in which the NTF and CTF heterodimerize [9–12]. This heterodimerization is a prerequisite for the endoproteolytic processing [13]. It has been proposed that the stable NTF:CTF heterodimer is the biologically active complex [14].

To date, the domains responsible for presenilin complex formation and other intramolecular interactions have not been reported. We previously characterized the *Drosophila* full-length presenilin (*Psn*) [15] and we now report the binding between several presenilin domains by two-hybrid analysis. Our data, also confirmed by the in situ split-ubiquitin assay support the predicted NTF:CTF heterodimerization and also reveal NTF:NTF and CTF:CTF homodimers. Furthermore, from the two-hybrid analysis and the glutathione *S*-transferase (GST) pull-down binding assay we infer that the NTF hydrophilic loop facing the ER between TMI and TMII accounts for the NTF:NTF interaction and that this binding is altered by FAD-linked presenilin mutations.

2. Materials and methods

2.1. DNA constructs

The entire sequence and six fragments of the *Drosophila* presenilin gene (*Psn*) were subcloned in-frame into the yeast two-hybrid pACT2 (prey) and pAS2-1 (bait) vectors (Matchmaker Yeast Two-hybrid system II, Clontech). The primers used for PCR amplification of each *Psn* fragment and their position with respect the protein are listed in Table 1.

For GST pull-down experiments, PSN HL1 (the 32 aa hydrophilic loop between TMI and TMII) was fused to GST (GST-HL1). The second construct containing the PSN-HL1 fused to the HA (hemagglutinin) epitope and GST (GST-HA-HL1) was obtained using a HA-HL1 fragment obtained from the HL1pACT2 construct.

Site-directed mutagenesis was performed by PCR amplification using the full-length *Psn* template as described [16]. Mutagenic oligonucleotides are listed in Table 1.

Split-ubiquitin constructs containing *Drosophila* PSN NTF (aa 1–322) and CTF (aa 321–541) were generated as follows: A yeast centromeric plasmid (derived from pRS415, kindly provided by B. Piña) containing the ADH1 promoter and termination expression cassettes was constructed to clone either PSN NTF or PSN CTF directly fused to Cub-ProtA-LexA-Vp16. The gene fusion Cub-ProtA-LexA-Vp16 was obtained from pRS375 (kindly provided by I. Stagljar). The fusions between PSN NTF and PSN CTF to Cub generated the peptide linkers GSTSSRVEGSTMSG and SSSRVESGGSTMSG, respectively. The fusion constructs containing NubG fused to PSN NTF and to PSN CTF were cloned into pRS396 (kindly given by I. Stagl-

*Corresponding author. Fax: (34)-93-4110969.
E-mail address: gemma@porthos.bio.ub.es (G. Marfany).

0014-5793/01/$20.00
PII: S0014-5793(01)02785-5

jar) by substituting ALG5-Nub as a cassette. The expression from these Nub-PSN-derived fusions was driven by the CUP1 promoter. The fusions NubG-PSN NTF and NubG-PSN CTF generated the short peptide linker IIEF.

The identity and reading frame of all DNA constructs was confirmed by sequencing with the Dye Terminator Cycle Sequencing Ready Reaction Kit (Perkin Elmer) and a 377 ABI PRISM sequencer.

2.2. Yeast two-hybrid assay

Yeast strains Y190 and CG-1945 were co-transformed with prey and bait plasmids derived from pACT2 and pAS2-1 using the standard lithium acetate procedure. Transformants were selected for growth on SD-His/-Trp/-Leu plates with 25 mM 3-aminotriazole for the Y190 strain and 5 mM for the CG-1945. Y190 transformants were assayed for β-galactosidase activity by filter-lift assay using X-gal as a substrate. Quantification of β-galactosidase activity was achieved by a liquid culture β-galactosidase assay using ONPG as substrate. Negative controls were performed using pLAM5' (Clontech) and empty prey and bait vectors. All protocols were according to the manufacturer's instructions (Clontech).

2.3. Split-ubiquitin assay

Yeast strain L40 was co-transformed with the corresponding Nub- and Cub- derived constructs using the lithium acetate procedure. Transformants were selected for growth on SD-His/-Trp/-Leu with 25 mM 3-aminotriazole and 0.2 mM Cu^{2+}.

2.4. Yeast protein extractions and immunoblotting

Detection of correct expression of GAL4-fusion proteins in the two-hybrid assay was performed by growing the corresponding clones bearing the two assayed constructs, until 0.4–0.6 OD. Protein extracts were obtained following the specifications of the plasmid supplier (Clontech), heated at 55°C, electrophoresed and immunodetected using the monoclonal antibody HA.11 (BAbCO) and a polyclonal antibody against GAL4-BD (Santa Cruz) for detecting GAL4-AD and GAL4-BD protein fusions, respectively. In the split-ubiquitin assays, yeast cells were grown in 25 ml of the corresponding rich or selective media up to 1 O.D., harvested by centrifugation, washed twice with 1 vol of distilled water and finally resuspended in 150 μl of cold lysis buffer (100 mM Tris–HCl, pH 7.5; 150 mM NaCl; 2 mM EDTA; 1% digitonin; 0.5% NP-40 and protease inhibitors). Cells were mechanically broken with glass beads and the protein extract was recovered after centrifugation (4500 rpm in a microfuge). After a second centrifugation (13 000 rpm in a microfuge) for 20 min, pellets and supernatants were treated separately. Pellets containing insoluble and membrane associated proteins were directly resuspended in protein loading buffer solution for SDS–PAGE gels, whereas supernatants were precipitated with 5 vol of cold acetone (1 h at −20°C), centrifuged, air-dried and resuspended in protein loading buffer solution. Protein samples were loaded onto an SDS–PAGE electrophoresis gel after heating for 15 min at 50°C, blotted onto a polyvinylidene fluoride (PVDF) membrane, immunodetected with Anti-ProtA (Sigma) and visualized using SuperSignal (Pierce) reagents.

2.5. In vitro binding assay

GST-HL1, GST-HA-HL1 and GST constructs (derived from pGEX4T-1) were transformed into BL21 cells. Cells were grown overnight at 37°C, diluted 1:10 and grown for 1 h at 30°C. After induction with 1 mM IPTG for 90 min, cells were sonicated and the fusion proteins were affinity-bound to glutathione Sepharose beads, following the manufacturer's instructions (Amersham Pharmacia Biotech). Purified HA-HL1 was obtained after thrombin digestion of the immobilized GST-HA-HL1 protein as described [17]. Approximately 2 μg of the immobilized GST and GST-HL1 proteins were mixed with HA-HL1 in 600 μl of Bead Binding Buffer (20 mM HEPES, pH 7.9, 100 mM KCl, 1 mM $MgCl_2$, 10 μM $ZnCl_2$, 0.5% Triton X-100, 10% glycerol, 2 mM dithiothreitol and 1 mM phenylmethylsulfonyl fluoride). After incubation for 2 h at 4°C under gentle mixing, beads were washed three times in 500 μl of Bead Binding Buffer, eluted in 2×Tris–tricine protein sample buffer and loaded onto a 20% SDS–polyacrylamide gel. The protein gels were blotted onto a PVDF filter, immunodetected with monoclonal antibody HA.11 (BAbCO) and visualized by enhanced chemoluminescence (Amersham Pharmacia Biotech).

3. Results and discussion

Positive NTF:CTF heterodimerization is shown (Fig. 1a), in agreement with previous findings on human and mouse cells mainly by co-immunoprecipitation and protein fractionation on glycerol velocity gradients [9,10,12,18,19]. This interaction occurred either in the absence or presence of an alternatively spliced exon [15] encoding 14 aa embedded in the cytoplasmic hydrophilic loop (HL6). Besides, the hydrophobic transmembrane domains of the NTF and CTF peptides did not interfere with transport to the nucleus nor with proper interaction as shown by the positive binding in the two-hybrid analysis (Fig. 1a), even though an ER location has been reported for these peptides. To identify the binding site for the NTF:CTF interaction, constructs encoding shorter peptide domains were analyzed. A shorter NTF containing the hydrophilic loop (N-loop, aa 1–100) interacted with either the HL6 cytosolic hydrophilic loop of CTF or the C-terminal hydrophobic segment (the last 38 aa), after TMVIII (C-loop) (Fig. 1a). Both interactions might be due either to a specific require-

Table 1
List of primers used in the experiments described in this work (PCR amplification of Psn-domains and site-directed mutagenesis)

Oligonucleotide	Sequence	First aa encoded
CompF	5′-GGAATTCATGGCTGCTGTCAATCT-3′	1
CompR	5′-CGGGATCCTATAAACACCTGCTTGGC-3′	541
NloopR	5′-CGGGATCCCCCGTATTTCAGGCCCTG-3′	100
HL1F	5′-GGAATTCAACTCCATCAGCTTCTAC-3′	123
HL1R	5′-CGGGATCCGGCACTCCAGAACTTAAC-3′	154
HL6F	5′-GGAATTCTCGCCAAGAGGACCCCTC-3′	285
Loop6R	5′-CGGGATCCGCCACGTTCTTCTTGCCC-3′	454
NterR	5′-CGGGATCCAACAGTGTTTACAAGTGC-3′	322
CterF	5′-GGAATTCACTGTTACGCCGCAGCAA-3′	321
CterHLF	5′-GGAATTCCGCAAGGCGCTACCCGCC-3′	503
Y137H	5′-CTATCTCCTCCACACACCTTTC-3′	site-directed mutagenesis
Y137C	5′-CTATCTCCTCTGCACACCTTTC-3′	site-directed mutagenesis
Y137P	5′-CTATCTCCTCCCCACACCTTTC-3′	site-directed mutagenesis
E142K	5′-ACCTTTCCATAAACAATCGCCCG-3′	site-directed mutagenesis
E142D	5′-ACCTTTCCATGATCAATCGCCCG-3′	site-directed mutagenesis
E142W	5′-ACCTTTCCATTGGCAATCGCCCG-3′	site-directed mutagenesis
T138N	5′-TCTCCTCTACAACCCTTTCCAT-3′	site-directed mutagenesis
P139L	5′-CCTCTACACACTTTTCCATGAA-3′	site-directed mutagenesis

Mutations are underlined.
F: Forward oligonucleotide; R: reverse oligonucleotide.

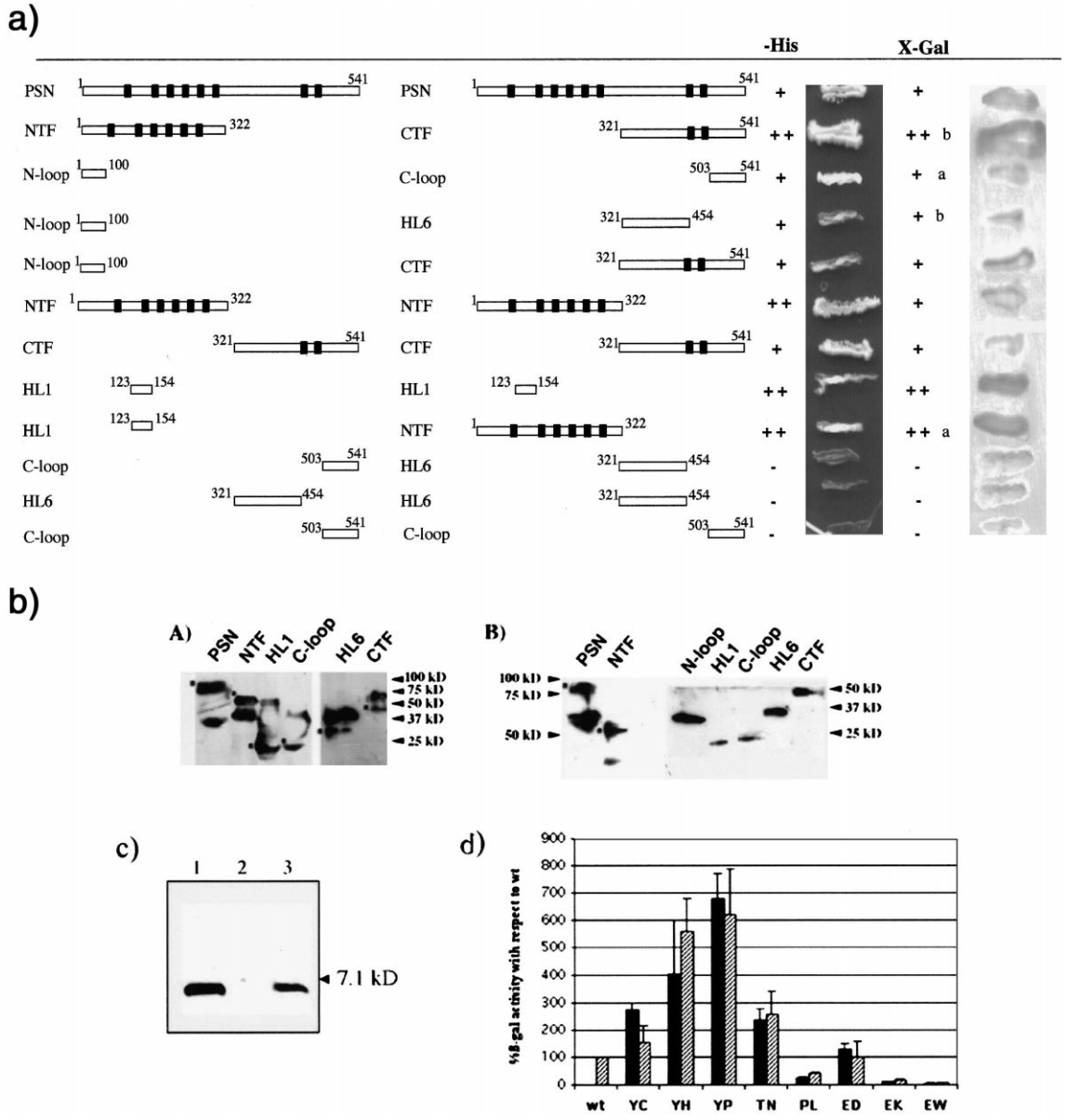

Fig. 1. a: Two-hybrid analyses of PSN fragments. The constructs encoding different domains of PSN listed were assayed in pairs (as shown). Histidine independent growth was tested in plates lacking histidine and supplemented with 5 mM 3-aminotriazole (3AT) in yeast strain CG-1945. β-Galactosidase activity was shown with the filter-lift assay and X-gal as substrate in yeast strain Y190. +,− indicate the strength of the interaction. a: reverse experiment gave inconsistent values; b: reverse confirmatory values were obtained. Black boxes depict transmembrane domains. b: Immunodetection of all the tested PSN fragments when fused to the GAL4-BD (A) and GAL4-AD (B) domains. The immunoblot of the PSN peptides fused to the GAL4 domains rendered the expected size band (indicated by an asterisk), although in some cases other bands were also detected, corresponding to protein aggregates or to protein degradation. c: In vitro binding assay. GST-HL1 and GST alone were bound to glutathione Sepharose beads and mixed with purified HL1-HA. After incubation and washes, samples were resolved on 20% Tris–tricine polyacrylamide gel, blotted onto a PVDF membrane and immunodetected with anti-HA. Lane 1: Purified HL1-HA (5% of the amount used in the binding assays; control); 2: GST alone (negative control), HL1-HA was not retained; 3: GST-HL1, retained HL1-HA. d: Quantification of β-galactosidase activity. Yeast strain Y190 co-transformed with mutant and wild-type (wt) HL1pAS or HL1pACT was grown on selective medium. β-Galactosidase activity was quantified using ONPG as substrate. Values obtained for each pair of constructs (five to 10 replicas) are represented with respect to wt HL1pAS/HL1pACT clones, which represent the 100% activity. Black bars show heterozygous combinations: pAS carried the mutant HL1 and pACT, the wt HL1. Striped bars show homozygous mutations: both HL1pAS and HL1pACT constructs bore the mutant versions of HL1.

ment for NTF:CTF binding or to a 'sticky' nature of the N-loop itself, as the interacting segments were very different in their hydropathic profile. Our data on other positive interactions of this N-loop with several PSN peptides (data not shown) would support the latter. An immunodetection showing correct expression of all the tested PSN peptides when fused to the GAL4-BD and GAL4-AD domains validated our previous results. (Fig. 1b).

We also tested NTF and CTF ability to form complexes other than the NTF:CTF heterodimer. The two-hybrid assay allowed to analyze NTF and CTF homodimerization, very difficult to detect otherwise. The strong interactions shown

suggested the formation of NTF:NTF and CTF:CTF homodimers (Fig. 1a). Again, the latter was unaffected by the 14 aa enclosed in the alternative exon. In order to identify the peptides responsible for NTF homodimerization, several shorter constructs were tested. Interestingly, the HL1 peptide corresponding to the 32 aa ER hydrophilic turn between TMI and TMII produced a clear HL1:HL1 homodimer (Fig. 1a), whereas the N-loop (first 100 aa) yielded inconsistent results and was not further considered. Additional positive and negative controls were assayed to confirm the specificity of all the interactions (Fig. 1a and data not shown). Finally, attempts to define the domains responsible for CTF:CTF homodimerization after dissecting CTF in several domains were not successful (Fig. 1a). These negative results were not due to incorrect expression of the fusion proteins as shown by immunodetection (Fig. 1b). As transmembrane domains had not been included in these constructs, their contribution to homodimer binding could not be discarded.

To confirm HL1:HL1 homodimerization, a GST pull-down assay was performed. Of the two GST-HL1 constructs, the prey contained an additional HA epitope fused to HL1 (GST-HA-HL1) to allow discrimination from GST-HL1 (bait). After binding to glutathione beads, the GST-HA-HL1 protein was proteolysed with thrombin and the isolated HA-HL1 peptide was incubated with matrix-bound GST-HL1 (bait). After immunodetection of HA-HL1 with an anti-HA antibody, the specificity of the HL1:HL1 interaction was shown (Fig. 1c).

Interestingly, nine FAD-linked missense mutations are clus-

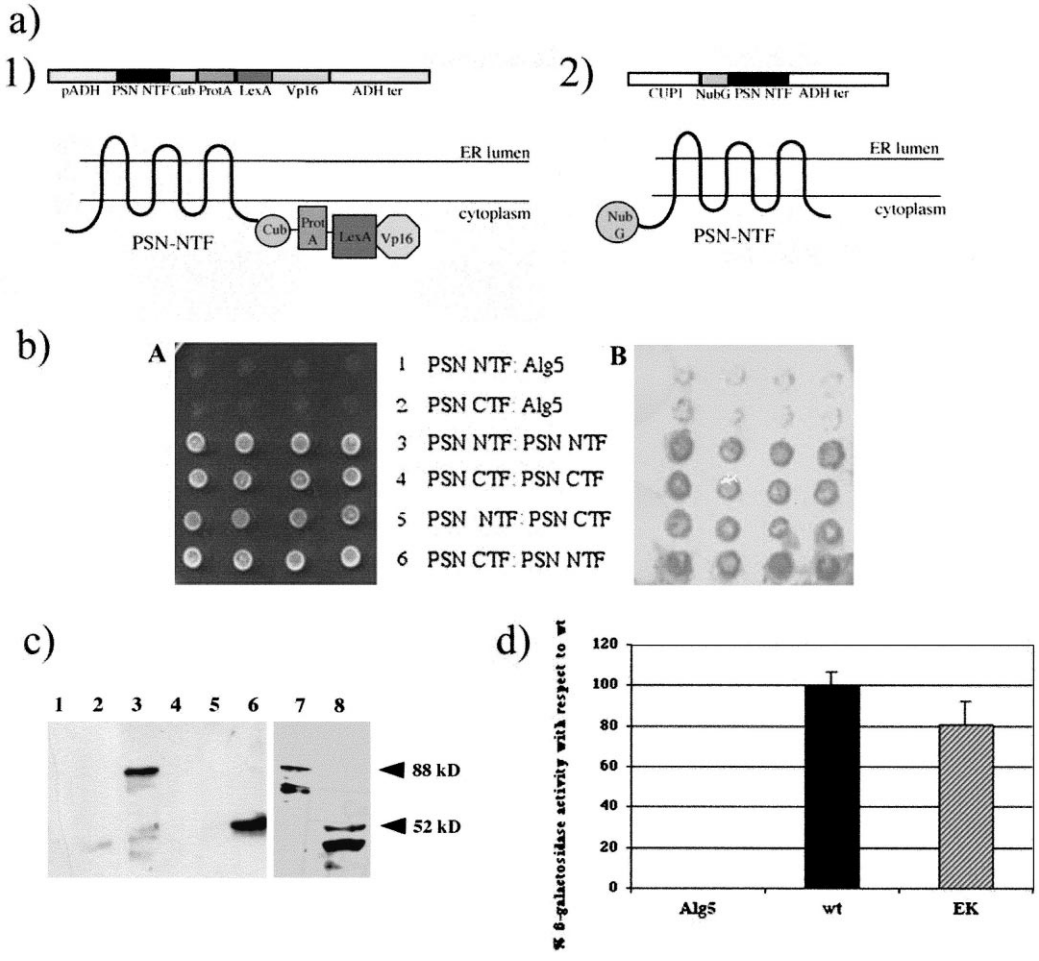

Fig. 2. a: The split-ubiquitin constructs (1) PSN NTF-Cub-ProtA-LexA-Vp16 and (2) NubG-PSN NTF were cloned in the yeast expression vectors pRS415 and pRS396, respectively. The topology of the fusion protein is also shown. Similar, PSN CTF constructs were also constructed to be tested in this assay (the figures are not depicted). The original split-ubiquitin constructs were kindly provided by I. Stagljar. b: The split-ubiquitin assay was performed by co-transformation of yeast strain L40 with the following pairs of fusion proteins: (1) NubG-Alg5 and PSN NTF-Cub-ProtA-LexA-Vp16 (negative control); (2) NubG-Alg5 and PSN CTF-Cub-ProtA-LexA-Vp16 (negative control); (3) NubG-PSN NTF and PSN NTF-Cub-ProtA-LexA-Vp16; (4) NubG-PSN CTF and PSN CTF-Cub-ProtA-LexA-Vp16; (5) NubG-PSN NTF and PSN CTF-Cub-ProtA-LexA-Vp16; (6) NubG-PSN CTF and PSN NTF-Cub-ProtA-LexA-Vp16. (A) Three days growth on SD-Leu/Trp/His+3-aminotriazole (3AT) 25 mM; (B) X-Gal filter-lift assay. Four different clones were tested for each group of constructs. c: Immunodetection of the split-ubiquitin protein products using anti-ProtA on a Western blot of the protein cell extracts separated in pellet (lanes 1, 3, 5 and 7) and soluble (lanes 2, 4, 6 and 8) fractions. Lanes 1 and 2: untransformed yeast strain L40 (negative control); lanes 3 and 4: yeast expressing the PSN NTF-Cub-ProtA-LexA-Vp16 protein where only the precursor peptide is produced; lanes 5 and 6: yeast co-expressing NubG-PSN NTF and PSN NTF-Cub-ProtA-LexA-Vp16 proteins, where after the interaction of both NTF fragments and reconstitution of ubiquitin, the ProtA-LexA-Vp16 peptide is cleaved off; lanes 7 and 8: yeast co-expressing NubG-mutant (EK) PSN NTF and wt PSN NTF-Cub-ProtA-LexA-Vp16 proteins, where due to impaired NTF interaction, the ProtA-LexA-Vp16 peptide is cleaved off less efficiently (some uncleaved precursor still remained in the insoluble fraction). d: Quantification of β-galactosidase activity using ONPG as substrate. Yeast strain L40 was co-transformed with PSN NTF-Cub-ProtA-LexA-Vp16 and EK or wild-type (wt) NubG-PSN NTF and grown on selective medium. Values for each pair of constructs (6 replicas) are represented with respect to wt (100% activity).

tered in the HL1 domain, affect seven out of the 32 aa, and five of those correspond to conserved residues between human and *Drosophila*. To determine whether these mutations alter the HL1:HL1 interaction, we reproduced each mutation by site-directed mutagenesis. Wild-type and mutated HL1 constructs were quantified for β-galactosidase activity on ONPG following the yeast two-hybrid analysis. The *Drosophila* mutations analyzed were Y138H (Y115 in human PS1), Y138C (Y115 in human PS1), T139N (T116 in human PS1), P140L (P117 in human PS1), E143D (E120 in human PS1) and E143K (E120 in human PS1), reviewed in [5]. We also assayed two additional mutations, whose severity was predicted on the basis of aa similarities [20,21]: Y138P and E143W. As expected, all mutations clearly affected the interaction, either increasing or decreasing the affinity of the binding (Fig. 1d). Homodimerization was similarly affected when mutants were in homozygous or heterozygous combination, in agreement with the dominant inheritance associated to these ADs causing alleles (Fig. 1d). Extreme interaction variations were observed with the predicted two more severe mutations Y138P and E143W (six-fold increase and 20-fold decrease, respectively). Secondary structure prediction of the HL1 segment by the network protein sequence analysis (http://pbil.ibcp.fr) identified an extended strand (residues 11–15 of HL1) amidst a coiled-coil segment. Introduction of FAD-linked mutations in HL1 affected the extension and location of the extended strand, therefore linking variations in binding affinity to secondary structure. Although in some cases we have found positive correlation between FAD-onset age and aa substitutions (Table 2), clear cut genotype–phenotype correlations could be blurred by the different genetic background of each patient, even in a single family. In the same way, other attempts to establish a relationship between amyloid Aβ42 peptide secretion and FAD age of onset have been unsuccessful [22].

Artefacts in the two-hybrid analysis could arise from incorrect protein folding or improper localization as they contain several highly hydrophobic domains and are usually anchored in the ER and Golgi. To discard this possibility, the yeast split-ubiquitin system, based on the reconstitution of a full-length ubiquitin from the N-terminal (Nub) and C-terminal (Cub) domains [23], was used to show that PSN NTFs and CTFs formed homo- and heterodimers when anchored in the ER. The Nub and Cub fragments were expressed as independent fusions with the pressumptive interacting proteins (Fig. 2a). In addition, the C-terminal ubiquitin moiety (Cub) was fused to an immunodetectable peptide (ProtA) and a transcription factor (LexA-Vp16) (Fig. 2a). Upon in situ protein–protein interaction, the reconstituted ubiquitin would be cleaved by the numerous cellular UBPs (ubiquitin specific proteases), and the reporter genes (in our case, *HIS3* and *lacZ*) would be activated by the released transcription factor. To avoid diffusion of uncleaved Cub-ProtA-LexA-Vp16 precursor into the nucleus, this gene fusion was inserted into a low-expression centromeric vector. This in vivo assay allows (a) proper subcellular localization of the proteins analyzed, (b) detection of homodimers without the need to use epitopes, (c) easy co-transfection and simultaneous protein expression and finally, (d) reliable quantification of the interactions of wild-type and mutant proteins by the use of sensitive reporters.

Table 2
Genotype–phenotype correlation between the mutation effect on the interaction and FAD-onset age

Mutation	Age at onset	β-Gal activity with respect to wild-type	
		heterozygous	homozygous
Y115C	42	×2.74	×1.53
Y115H	36	×4.00	×5.60
T116N	35–41	×2.35	×2.56
P117L	24–31	×0.26	×0.40
E120D	43–48	×1.29	×1.00
E120K	35–39	×0.10	×0.16

Interaction value between wild-type constructs is arbitrarily considered as 1.

Yeast strain L40 co-transformed with the corresponding PSN-derived fusion constructs containing Cub-ProtA-LexA-Vp16 and NubG (Fig. 2a), grew on plates lacking tryptophan, leucine and histidine and gave blue staining in X-gal assays (Fig. 2b). Our results clearly confirmed positive NTF:NTF, CTF:CTF and NTF:CTF when anchored in the ER (Fig. 2b). Further, the specificity of the interaction was confirmed by the absence of growth in yeast co-transformed with either PSN NTF-Cub-ProtA-LexA-Vp16 or PSN CTF-Cub-ProtA-LexA-Vp16 and another yeast ER transmembrane protein (Alg5-NubG) [23] (Fig. 2b, negative controls). The cleavage of the ProtA-LexA-Vp16 transcription factor by UBPs after NubG–Cub reconstitution was clearly confirmed by immunodetection (Fig. 2c). The cleaved ProtA-LexA-Vp16 product (52 kDa) was detected in the soluble protein fraction, while the uncleaved precursor PSN NTF-Cub-ProtA-LexA-Vp16 (88 kDa) was only present in the pellets containing insoluble or membrane associated proteins, thus indicating a correct localization of the presenilin fusion in the ER. This result agreed with previous reports showing that heterologous presenilins bound the ER membrane in yeast [24,25]. Only the uncleaved precursor PSN NTF-Cub-ProtA-LexA-Vp16 was detected in yeast transformed with this construct alone (Fig. 2c, compare lanes 3 and 4). In contrast, when yeast was co-transformed with the gene fusions containing NTF interacting partners, the cleaved transcription factor clearly appeared in the soluble fraction (Fig. 2c, compare lanes 6 and 8). In addition, we also assessed the effect of FAD-linked mutations in NTF:NTF in situ homodimerization, by introducing the substitution E143K (corresponding to human PS1 E120K Alzheimer's mutation) using site-directed mutagenesis. Clearly, the NTF:NTF interaction was impaired by the mutation, as the cleavage from the precursor was less efficient and some uncleaved precursor remained in the insoluble fraction (Fig. 2c, lanes 7 and 8). The effect of this mutation on NTF homodimerization was further confirmed by quantification of β-galactosidase activity. The mutant NTF clearly showed a decrease (80% of lacZ activity after six replicas) in binding affinity with respect to wild-type NTF (Fig. 2d). The higher decrease in the mutant HL1:HL1 interaction (detected by two-hybrid analysis, Fig. 1d) than in the mutant NTF:NTF (detected by the split-ubiquitin assay, Fig. 2d) could be explained by a more restricted conformation of the HL1 domain when flanked by the two transmembrane helices of the NTF peptide. In fact, if we consider that mutations causing AD are neither lethal nor strongly deleterious, a large effect of the mutations on presenilin function should not be expected.

According to our data, interactions between the different subdomains (NTF:CTF, NTF:NTF, CTF:CTF) would be

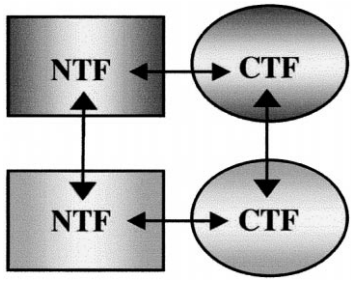

Fig. 3. Diagram showing an hypothetic presenilin functional unit with the observed interactions among NTFs and CTFs.

required for the correct assembly of a hypothetic tetramer, with two NTFs and two CTFs instead of a single NTF:CTF heterodimer (Fig. 3), strongly suggesting a new organization for the presenilin functional complex. Irrespective of whether the presenilin is the long-sought γ-secretase or a necessary partner for the γ-secretase activity, our hypothesis supports the notion that formation of the presenilin tetramer would be a crucial step for the assembly or stability of the high molecular weight presenilin–γ-secretase complex. Subtle changes in presenilin binding affinity caused by some FAD-linked mutations could result in dysfunction of the γ-secretase activity, thus triggering the cellular processes eventually leading to AD.

Acknowledgements: We thank the Serveis Científico-Tècnics de la Universitat de Barcelona for the use of the 377 ABI PRISM and Robin Rycroft for revising the English version. We are very grateful to B. Piña (CSIC, Barcelona) for the gift of plasmid pRS415 and to I. Stagljar (Institute of Veterinary Biochemistry, Zurich) for the gift of pRS304-, pRS305- and pRS314-derived constructs and helpful comments on the split-ubiquitin system. S.C. was a recipient of a fellowship from the CIRIT (Generalitat de Catalunya). This study was funded by BIO4-CT97-2123, PB96-0220 and PGC99-0168 (Ministerio de Ciencia y Tecnología) to R.G.-D.

References

[1] Kovacs, D.M. and Tanzi, R.E. (1998) Cell. Mol. Life Sci. 54, 902–909.
[2] Cruts, M. (1998) Hum. Mut. 11, 183–190.
[3] Cruts, M., Hendriks, L. and Van Broeckhoven, C. (1996) Hum. Mol. Genet. 5, 1449–1455.
[4] Drouet, B., Pincon, R.M., Chambaz, J. and Pillot, T. (2000) Cell. Mol. Life Sci. 57, 705–715.
[5] Fraser, P.E., Yang, D.S., Yu, G., Levesque, L., Nishimura, M., Arawaka, S., Serpell, L.C., Rogaeva, E. and St George-Hyslop, P. (2000) Biochim. Biophys. Acta 1502, 1–15.
[6] Ratovitski, T., Slunt, H.H., Thinakaran, G., Price, D.L., Sisodia, S.S. and Borchelt, D.R. (1997) J. Biol. Chem. 272, 24536–24541.
[7] Thinakaran, G., Borchelt, D.R., Lee, M.K., Slunt, H.H., Spitzer, L., Kim, G., Ratovitsky, T., Davenport, F., Nordstedt, C., Seeger, M., Hardy, J., Levey, A.I., Gandy, S.E., Jenkins, N.A., Copeland, N.G., Price, D.L. and Sisodia, S.S. (1996) Neuron 17, 181–190.
[8] Thinakaran, G., Harris, C.L., Ratovitski, T., Davenport, F., Slunt, H.H., Price, D.L., Borchelt, D.R. and Sisodia, S.S. (1997) J. Biol. Chem. 272, 28415–28422.
[9] Yu, G., Chen, F., Levesque, G., Nishimura, M., Zhang, D.-M., Levesque, L., Rogaeva, E., Xu, D., Liang, Y., Duthie, M., St George-Hyslop, P.H. and Fraser, P.E. (1998) J. Biol. Chem. 273, 16470–16475.
[10] Capell, A., Grunberg, J., Pesold, B., Diehlmann, A., Citron, M., Nixon, R., Beyreuther, K., Selkoe, D.J. and Haass, C. (1998) J. Biol. Chem. 273, 3205–3211.
[11] Thinakaran, G., Regard, J.B., Bouton, C.M., Harris, C.L., Price, D.L., Borchelt, D.R. and Sisodia, S.S. (1998) Neurobiol. Dis. 4, 438–453.
[12] Seeger, M., Nordstedt, C., Petanceska, S., Kovacs, D.M., Gouras, G.K., Hahne, S., Fraser, P., Levesque, L., Czernik, A.J., George, H.P., Sisodia, S.S., Thinakaran, G., Tanzi, R.E., Greengard, P. and Gandy, S. (1997) Proc. Natl. Acad. Sci. USA 94, 5090–5094.
[13] Saura, C.A., Tomita, T., Davenport, F., Harris, C.L., Iwatsubo, T. and Thinakaran, G. (1999) J. Biol. Chem. 274, 13818–13823.
[14] Yu, G., Chan, F., Nishimura, M., Steiner, H., Tandon, A., Kawarai, T., Arawaka, T., Supala, A., Song, Y.-Q., Rogaeva, E., Holmes, E., Zhang, D.M., Milman, P., Fraser, P.E., Haass, C. and St. George-Hyslop, P. (2000) J. Biol. Chem. 275, 27348–27353.
[15] Marfany, G., DelFavero, J., Valero, R., DeJonghe, C., Woodrow, S., Hendriks, L., Van Broeckhoven, C. and Gonzàlez-Duarte, R. (1998) J. Neurogenet. 12 (1), 41–54.
[16] Cols, N., Marfany, G., Atrian, S. and Gonzàlez-Duarte, R. (1993) FEBS Lett. 319, 90–94.
[17] Ausubel, F.M., Brent, R., Kingston, R.E., Moore, D.D., Seidman, J.G., Smith, J.A., and Struhl, K. (1994) Current Protocols in Molecular Biology 2, John Wiley and Sons, Inc., New York
[18] Steiner, H., Capell, A., Pesold, B., Citron, M., Kloetzel, P.M., Selkoe, D.J., Romig, H., Mendla, K. and Haass, C. (1998) J. Biol. Chem. 273, 32322–32331.
[19] Beher, D., Elle, C., Underwood, J., Davis, J.B., Ward, R., Karran, E., Masters, C.L., Beyreuther, K. and Multhaup, G. (1999) J. Neurochem. 72, 1564–1573.
[20] Schwartz, R.M. and Dayhoff, M.O. (1978) Atlas Protein Seq. Struct. 5, 353–358.
[21] Feng, D.F., Johnson, M.S. and Doolittle, R.F. (1985) J. Mol. Evol. 21, 112–125.
[22] Citron, M., Eckman, C.B., Diehl, T.S., Corcoran, C., Ostaszewski, B.L., Xia, W., Levesque, G., St. George-Hyslop, P., Younkin, S.G. and Selkoe, D.J. (1998) Neurobiol. Dis. 5, 107–116.
[23] Stagljar, I., Korostensky, C., Johnsson, N. and teHeesen, S. (1998) Proc. Natl. Acad. Sci. USA 95, 5187–5192.
[24] Evin, G., Le, B.D., Culvenor, J.G., Galatis, D., Weidemann, A., Beyreuther, K., Masters, C.L. and Cappai, R. (2000) NeuroReport 11, 405–408.
[25] Song, S.C., Ohba, M., Saito, Y., Honda, T., Takashima, A. and Takahashi, H. (2000) Neurosci. Lett. 282, 65–68.